Machine Learning approach for Numerical technique for classifying Cysts and Malignant Tumors in Breast

Akshara Makrariya (akshara.makrariya@vitbhopal.ac.in)
VIT Bhopal
Rabia Musheer
VIT Bhopal

Research Article

Keywords: Benign Disorders, Finite Element method, Thermal Disturbances, Artifical Neural Network (ANN), Support Vector Machine (SVM), Random Forest (RF)

Posted Date: May 18th, 2022

DOI: https://doi.org/10.21203/rs.3.rs-1640235/v1

Machine Learning approach for Numerical technique for classifying Cysts and Malignant Tumors in Breast

Akshara Makrariya[1], Rabia Musheer Aziz[2],

[1,2] Department of Mathematics, VIT Bhopal University
Bhopal- Indore Highway, Kothrikalan, Sehore,-466116 (M.P.) INDIA

Abstract: *Tumor is an abnormal tissue which can be appeared at any part of the body. It can be classified to either benign or malignant. One of the most common women's tumors that infest the breast. Various benign disorders like development of cysts in woman's breast occur due to hormonal changes and are at the risk of becoming malignant. A number of thermal models are reported to differentiate between normal and malignant tissues of breast. But no thermal model is reported in study the effect of benign disorders on the literature to distinguish between benign and malignant disorders in woman's breast. An attempt has been made in this paper to study the thermal disturbances caused by cysts and malignant tumors in the fat tissues of woman's breast. The model is developed for a two-dimensional steady state case using penne's bio heat equation and incorporating parameters like thermal conductivity, blood mass flow rate and self-controlled metabolic heat generation. The appropriate adiabatic boundary conditions have been framed for various environmental conditions. The finite element method has been employed to obtain the solution. The results have been obtained for different sizes of spherical shaped cysts and different depth of tissues in hemispherical shaped woman's breast. The relation of size and position of the cysts have been studied with the thermal distribution in various tissues layers of the woman's breast. The comparison of thermal profiles for cysts and malignant tumors in woman's breast has been performed. A contrast in thermal behavior of cyst and malignant tumor in woman's breast is observed which can be useful to distinguish between the malignant tumor and cyst in woman's breast to prevent false positive test for malignant tumor. Accordingly, this study found that there are various factors that could affect the cancer classification and prediction. Therefore in this study, Breast cancer data classification have been done using three classification techniques which*

are Artifical Neural Network (ANN), Support Vector Machine (SVM), and Random Forest (RF) in order to improve the performance of the model trained the model with selected features according to the analysis done.

Keywords: *Benign Disorders; Finite Element method; Thermal Disturbances; Artifical Neural Network (ANN); Support Vector Machine (SVM); Random Forest (RF).*

1. INTRODUCTION

Breast is without significant veins and considered as practically homogenous in nature. Breasts comprise of lobules and conduits encompassed by glandular, stringy and greasy tissue. The surprising knots happen in numerous lady's breast during their lives and just a little part of these bumps are malignant growth [1]. The sore is a typical wellspring of breast knots which happens in around one of third of menopausal ladies [2]. The 80% of these irregularities discovered in lady's breast are to be considerate. The pimples can create in it is possible that one or the two breasts normally with the progressions happening in breast because old enough and typical changes in hormonal levels [3]. Growths are kindhearted liquid filled sacks with a little danger of being harmful. For some ladies, their greatest worry about a growth is that it is, or will become, malignancy [4]. Blisters are not malignant growths. Breast malignancy is the second most basic disease among ladies with almost 1.7 million new analyzed cases as announced as of late. Indeed, even with cutting edge determination strategies death rate stays around 12.5%. Quite possibly early analysis of the infection may improve the endurance rate [5].

The breast growths can create at whatever stage in life, however are generally basic in ladies more than 35 and grow all the more frequently as ladies draw nearer to the menopause and normally stop once a lady has experienced the menopause [6]. Breast sores can feel delicate or hard and can be of any size, going from a couple of millimeters to a few centimeters. Pimples normally become recognizable as a bump in the breast are found by chance during a standard screening mammogram (breast x-beam) or while having examinations at a breast center for another explanation [7, 8].

In spite of the fact that mammography, the current breast disease screening methodology is compelling, it has a few impediments, for example, radiation peril, significant expense for a screening apparatus and awkward technique. It is assessed that 1 of every 2 ladies will have in any event 1 bogus positive mammogram result, and 1 out of 5 ladies will have at any rate 1 bogus positive clinical breast assessment result [9, 10]. This might be because of failure of mammography to separate the anomalies when the densities of tissues are high, especially in thick breast tissues [11, 12]. Consequently, there is a requirement for a powerful screening device that is non-contact, non-obtrusive, and easy and radiation free, for example, clinical thermography to analyze the considerate changes like growths and harmful changes like malignancy in lady's breast [13, 14]. The investigation of warm conduct of blisters and harmful tumors in ladies' breast can be helpful for creating conventions for conclusion by thermo realistic ways to deal with recognize

growths and threatening tumors so as to forestall bogus positive tests for dangerous tumors [15-17].

Ongoing advances in infrared camera innovation and progress in mechanized picture handling frameworks has expanded the extension for improvement of breast thermography [18, 19]. Subsequently, a machine learning model based reproduction of temperature appropriation in ordinary, amiable and anomalous tissues is needed to comprehend and improve the demonstrative significance of infrared imaging framework [20, 21].

When all is said in done, Penne's profile heat condition is utilized to display the temperature dissemination in the human body tissues. Different models recommended have been accounted for as an improvement to penne's model that incorporate continuum models given by J Hristov et. al. [22]. Prior Patterson made trial examinations to get temperature profiles in the human body tissues. Some hypothetical work is accounted for during the most recent couple of a very long time by Cooper and Trezek to examine the temperature circulation in the human fringe locale under ordinary natural and physiological conditions [23]. Various researchers recently made endeavors to contemplate issues of temperature appropriation in the dermal locales of the human body including anomalies like tumors [24-26]. Taylor et.al, created warm models of human appendages for one and two - dimensional consistent state cases under ordinary physiological and natural conditions [27]. Abaci et. al, created one, two and three - dimensional limited component models to examine warm examples in the dermal layers of human appendages with and without tumors [28]. Some of the researcher explored the metabolic warmth age in breast tumors utilizing infrared pictures and mathematically recreating a disentangled breast model and a malignant tumor [29, 30]. Azzam, et. al., has introduced a review of hypothetical and clinical parts of thermography stressing the requirement for advancement of standard methodology to acquire and dissect the thermograms [31]. The absence of these standard strategies is one of the bottleneck is making thermography as a generally utilized procedure. Yuanni, et. al, performed warm recreation of breast tumors of different sizes to decide the scope of size and profundity of tumor in breast which can be identified with the accessible thermographic innovation [32]. No model is accounted for to recognize warm conduct of blisters and harmful tumors in ladies' breast. Here Penne's profile heat condition has been utilized to propose a model to recognize warm conduct of blisters and harmful tumors in lady's breast. It is comprehended utilizing limited component strategy and reproductions are completed for differed range and profundity of Cysts.

A. The objective of the paper

- To proposed the thermal model that effect of benign disorders to distinguish between benign and malignant disorders in woman’s breast.
- To study the thermal disturbances caused by cysts and malignant tumors in the fat tissues of woman’s breast.

- To study the relation of size and position with the thermal distribution in various tissues layers of the woman's breast by using finite element method.
- To improve the performance of the various classification model by using selected features of breast cancer data according to the done analysis.

B. Paper Organization

Thus, this article developed the model for thermal disturbances caused by cysts and malignant tumors in the fat tissues of woman's breast with a two-dimensional steady state case using penne's bio heat equation and incorporating parameters like thermal conductivity, blood mass flow rate and self-controlled metabolic heat generation. The appropriate adiabatic boundary conditions have been framed for various environmental conditions. The finite element method has been employed to obtain the solution. The rest of the paper is organize as follow: I) Introduction, II) Proposed Mathematical Model, III) Experimental Setup, IV) Experimental Results &. Discussion V) Machine Learning Validation VI) Conclusion.

2. Mathematical Model

The partial differential equation [24] for temperature distribution in living tissues for a two - dimensional steady state case in spherical coordinates is given by [33, 34]:

$$\frac{1}{r^2}\frac{\partial}{\partial r}\left(Kr^2\frac{\partial T}{\partial r}\right)+\frac{1}{r^2\sin\theta}\frac{\partial}{\partial\theta}\left(K\sin\theta\frac{\partial T}{\partial\theta}\right)+m_b c_b\left(T_A-T_v\right)+S=0 \tag{1}$$

The external surface of the hemispherical district is presented to the climate and warmth misfortune at this surface happens principally because of conduction, convection, radiation, and vanishing. Subsequently the limit condition forced at the external surface is given by

$$-K\frac{\partial T}{\partial r}=h\left(T-T_a\right)+LE \quad at \quad r=r_n \quad , \quad \theta\in\left(0,\pi\right) \tag{2}$$

Here for female body organs, *E and h* are given by [8]:

$$E=8.47\times10^{-5}\left(0.1\times T_0+0.7\times T_b\right)-36.6^{\circ}C \tag{2a}$$

$$h=1.32(T_w-T_a/2.r_5)^{1/4} \quad w/m^2{}^oC \tag{2b}$$

The Dirichlet condition at the inner boundary is imposed for two cases as given below:

2.1 Type-1 Boundary Condition:

At medium and higher atmospheric temperatures, the inner surface is maintained at a uniform body core temperature T_b . Hence the Dirichlet condition at inner boundary is given by

$$T(r,\theta) = T_b \;\; at \;\; r = r_0 \tag{3}$$

Where is r_0 the radius of core of the breast

2.2 Type -II Boundary Condition:

The shell temperature of female breast is variable along rakish heading θ during low air temperatures. The blood in the center of the storage compartment streams at body center temperature 370C through the supply routes of female breast. This warm blood chills off while arriving at boundaries some portion of breast losing warmth to the encompassing tissues of the bosom. This blood gets back from limits of breast at lower temperature then the body center temperature through the veins to the center of the storage compartment. Subsequently the limit condition forced is given by:

$$T(r,\theta) = F(\theta) \qquad at \;\; r = r_0 \tag{4a}$$

Where $F(\theta) = b_1 + b_2\theta + b_3\theta^2$

and $T(r_0,\theta) = \alpha_1 \;\; at \;\; \theta = 0$

$$\begin{aligned} T(r_0,\theta) &= \alpha_2 \;\; at \;\; \theta = \pi/2 \\ T(r_0,\theta) &= \alpha_3 \;\; at \;\; \theta = \pi \end{aligned} \tag{4b}$$

Here α_1 and α_3 are the temperatures of the portion of core of the breast near the trunk and so taken to be capable the body core temperature T_b. Here α_2 is that the temperature of the acute a part of the breast core ($\theta = \pi/2$) at a radial distance r_0 from the trunk and is usually under α_1, and α_3, at low atmospheric temperature. The values of the constants b_1, b_2 and b_3 are determined by using conditions (4b).

The normal tissues of breast have self-controlled metabolic activity which is expressed as [36,37]:

$$S = \overline{S}\left[1 + Q_d\left(T_b - T\right)\right], \text{ where } Q_d = \frac{2}{T_a + T_b}$$

In order to make the model non-dimensional the following scaling of parameters is used:

$$U=\frac{T_b-T}{T_b}, T=T_b\left(1-U\right),\quad U_A=\frac{T_b-T_A}{T_b}, T_A=T_b\left(1-U_A\right),\qquad U_V=\frac{T_b-T_V}{T_b}, T_V=T_b\left(1-U_V\right)$$

$$T_a=T_b\left(1-U_a\right)$$

$$r=r'r_n \Rightarrow r'=\frac{r}{r_n},\quad \theta=\theta'\pi \Rightarrow \theta'=\frac{\theta}{\pi},$$

Using these parameters in equation (1), we get non-dimensional form of the equation is:

$$\frac{\pi^2}{r'^2}\frac{\partial}{\partial r'}\left(Kr'^2\frac{\partial U}{\partial r'}\right)+\frac{1}{r'^2\sin(\theta'\pi)}\frac{\partial}{\partial\theta'}\left(K\sin(\theta'\pi)\frac{\partial U}{\partial\theta'}\right)+M\left(U_V-U_A\right)+S^*=0 \tag{5}$$

where
$$M=m_b c_b r_n^2\pi^2$$
$$S^*=\overline{S}\left[1+Q_d U T_b\right]r_n^2\pi^2$$

$S''=\eta S$ and $Q_d=0$ in malignant tissues η is parameter which represents ratio of metabolic activity in tumor and normal tissues , and the metabolic activity in tumors is found to vary between 1 to 7 times of that in normal tissues

The non- dimensional form of boundary conditions (2) ,(3) and (4) are given by:

$$-K\frac{\partial U}{\partial r'}=h^*\left(U-U_a\right)+L^*E^*,\qquad r=r_n\ \&\ \theta\in\left(0,\pi\right) \tag{6}$$

$hr_n=h^*$ and $E^*=Er_nT_b$. Hence boundary condition (6) can be written as:

and $\quad U=\frac{T_b-T}{T_b}=0\quad$ at = $\quad r'=r_0/r_n$ (7)

$$U\left(r_0,\theta'\right)=G\left(\theta'\right)$$
$$G\left(\theta'\right)=b_1+b_2\theta'+b_3\theta'^2$$
$$U\left(r_0,\theta'\right)=\chi, at\theta'=0 \quad \text{at} \quad r'=r_0/r_n \tag{8}$$
$$U\left(r_0,\theta'\right)=\delta, at\theta'=1/2$$
$$U\left(r_0,\theta'\right)=\mu, at\theta'=1$$

3. Experimental Setup

The inner core consists of blood vessels, lobes and glandular tissues. The first four layers above the core are muscles. Above the muscles there are three layers of glands. Above the glands the fat region is divided in to four layers. The breast fat is covered by four layers of skin and sub dermal tissues. A spherical shaped lump is assumed to be present in the fat layers. Initially this lump

assumed to be cyst and alternatively this lump is assumed malignant tumor. The whole region is divided into 560 coaxial circular sector elements and 615 nodes.

The equation (5) along with the boundary conditions (6) (7) and (8) in the variational form is written as given below:

$$I^{(e)} = \frac{1}{2}\iint \left[K^{(e)}\pi^2 r'^2 \left(\frac{\partial U^{(e)}}{\partial r'}\right)^2 + K^{(e)}\left(\frac{\partial U^{(e)}}{\partial(\theta'\pi)}\right)^2 + \left\{M^*\left(U_V^e - U_A^{(e)}\right) + S^{*(e)}\right\} U^{(e)} r'^2 dr' d(\theta'\pi) \right]$$

$$+ \frac{\lambda^{(e)}}{2}\int_{\theta_j}^{\theta_l'} \left\{ h^*\left(U^{(e)} - U_a\right)^2 + 2L^* E^* U^{(e)} \right\} r'^2 d(\theta'\pi) \quad for \quad e = 1(1)560 \qquad (9)$$

Here we assume non dimensionlized arterial blood temperature equal to the average of non dimensionlized nodal temperatures of the previous element along radial direction as the arterial blood will enter the eth element from its previous element below it and the blood will have almost average temperature of its previous element because blood gives heat to the element from which if passes and cools down to almost same temperature of that element. In the same way the venous blood temperature is also taken as average of nodal temperatures of element from which it is coming in to next element.

Here: $U_A^{(e)} = \left(\frac{U_i + U_j + U_k + U_l}{4}\right)^{(e-1)}$ and $U_A^{(e)} = \left(\frac{U_i + U_j + U_k + U}{4}\right)^{(e-1)}$

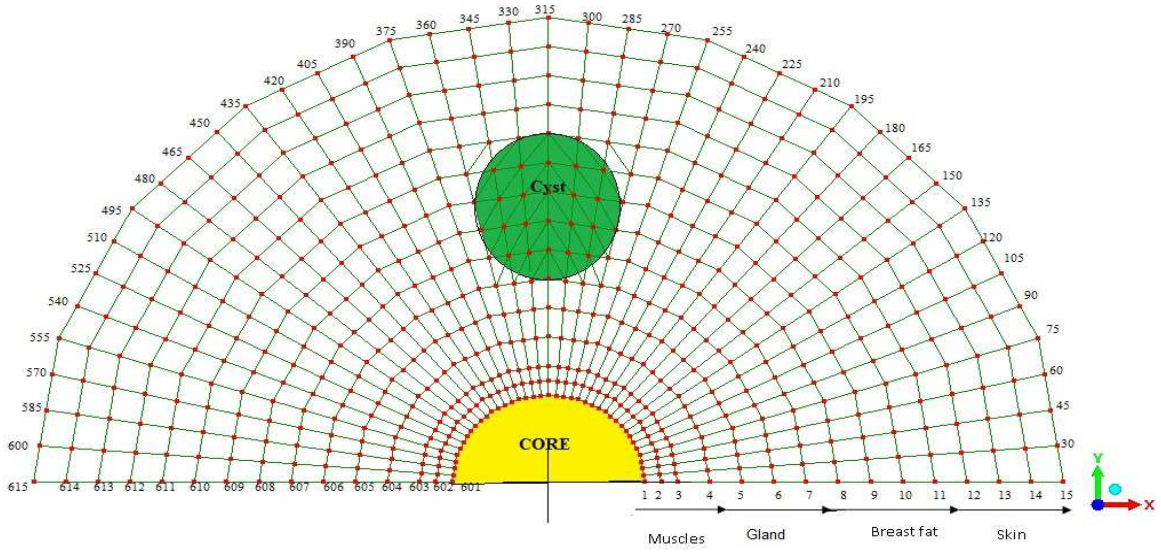

Fig.1. *Element wise discretization of woman's Breast Involving Cysts*

The following bilinear shape function for variation of temperature within each element has been taken as:

$$U^{(e)} = c_1^{(e)} + c_2^{(e)} r' + c_3^{(e)} \theta' + c_4^{(e)} r' \theta' \tag{10}$$

$$U^{(e)} = U_p \ , \ P = i, j, k, l \tag{11}$$

$$I^{(e)} = \sum_{e=1}^{N} I^{(e)} \tag{12}$$

$$\frac{dI}{d\overline{U}} = 0 \tag{13}$$

Where

$$\overline{U} = \begin{bmatrix} U_1 & U_2 & U_3 & - & - & - & - & U_{615} \end{bmatrix}$$

$$[X]_{615\times615} \left[\overline{U_{615\times1}} \right] = [Y]_{615\times1} \tag{14}$$

The Gauss elimination method has been used to obtain the solution of (14). A computer program in MATLAB is developed to find numerical solution to the entire problem.

4. Numerical Results &. Discussion

The numerical results are obtained by using the values of physical and physiological constant given in Table: 1

Table .1: The value for physical and physiological constants [43]

S.No.	***Tissues***	***K (W/cm°C)***	***ρ(g/cm³)***	***c_b (J/g °C)***	***S (W/cm³)***	***m_b (ml/S)***
1	Bone	75	135700	17	0	0
2	Muscle	42	108500	3768	68400	0.00018
3	Fat	16	85000	23	5800	0.00009
4	Skin	47	108500	368	36800	0.0001
5	cysts	56	0	0	0	0

The reenactment was performed for N=560 components at first. On the other hand for N=1120, 2240 and 4480 components. We get a temperature of 32.5666 at hub number 352 in blisters for model with N=560 components and temperature 32.5676 at hub number 697 in sores for model with N=1120 components. The mistake is [(32.2676 - 32.2666)/32.2676] *100 which works out to be 27x 10-6 % as it were. For better lucidity we take just the proportion of four decimal focuses (0.2666/0.2676) * 100=99.62% and call this term as certainty level. A certainty level of 100 infers that an immersion point has reached. In this work, we have utilized N=560 components as the

quantity of components in our model as we can securely say that outcomes are work unfeeling at this number. The constants (i=1(1)15) can be allocated any worth relying on specific example of tissues layers under examination. The outcomes are processed for following thickness of bosom layers is [8]:

For Case 1: Diameter of cyst 8.4 mm, Area 55.3896 mm^2, Circumference= 26.376 mm.

For Case 2: Diameter of cyst 12 mm, Area = 113.04 mm^2, Circumference= 37.68 mm.

For Case 3: Diameter of cyst 15 mm, Area = 176.625 mm^2, Circumference= 47.1 mm.

For Case small cyst: Diameter of cyst 2 mm, Area = 3.14 mm^2, Circumference= 6.28 mm

The cyst is taken between $\theta = 75^0$ and $\theta = 105^0$ in the fat layers of breast.

For Variable limit condition the accompanying arrangements of temperatures have been expected at inward limit. The mathematical outcomes have been figured and diagrams are plotted for the various instances of climatic temperature and various estimations of pace of dissipation [26]. The figure 3, 4, and 5 plotted for various sizes of blisters. In figure 3, 4 and 5 it is seen that the temperature falls pointedly in the blisters and tissues around the sores in the female breast. The greatest fall in the temperature is seen in the focal piece of the growths. The incline of the bend changes at the intersection of blisters and typical tissues of the female breast. The greatest temperature aggravations are seen in the growth district. This is because of the non-attendance of metabolic movement in the growths. The figure - 6 shows the examination of temperature dissemination in the focal piece of the pimples and threatening tumor $for\ \eta =$ 3.0 with ordinary tissues of female breast for $Ta = 230C, gm/cm2min,$ and Type-I limit condition at $\theta = \pi/2$. We see that temperature falls continuously up to $r = 6\ cm$ in fat layers of female breast and afterward falls strongly from 6.4 cm. up to $r = 6.9\ cm$. For ordinary tissues of female breast yet at the point $r = 6.6\ cm$. the incline of the bend changes for both harmful tumor and pimples. If there should be an occurrence of blisters we watch the further fall in temperature when contrasted with that for ordinary tissues in figure-6 while for dangerous tumor we watch the height in temperature profiles over.

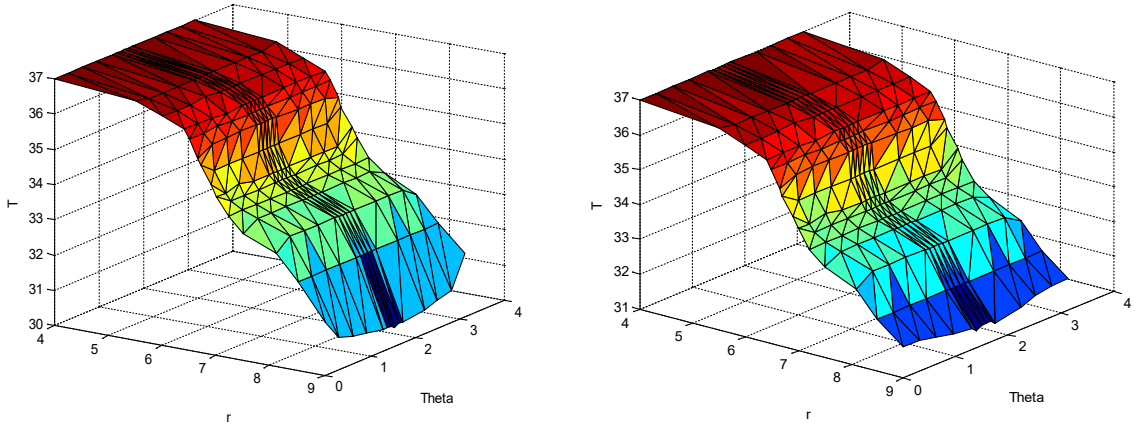

Fig.2. *Temperature distribution in Cysts in fat layers of Female breast for T_a=23^{0}C, $E = 0.24 \times 10^{-3}$ gm/cm^{2}min, and Type-I boundary condition and case -2*

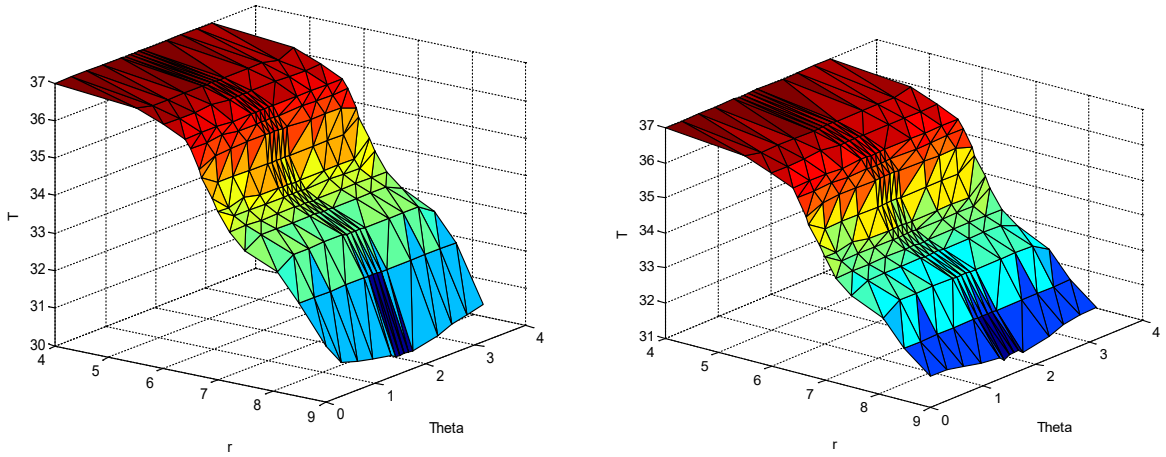

Fig.3. *Temperature distribution in Cysts in fat layers of Female breast for T_a=23^{0}C, $E = 0.24 \times 10^{-3}$ gm/cm^{2}min, and Type-I boundary condition and case -3 and case - 1*

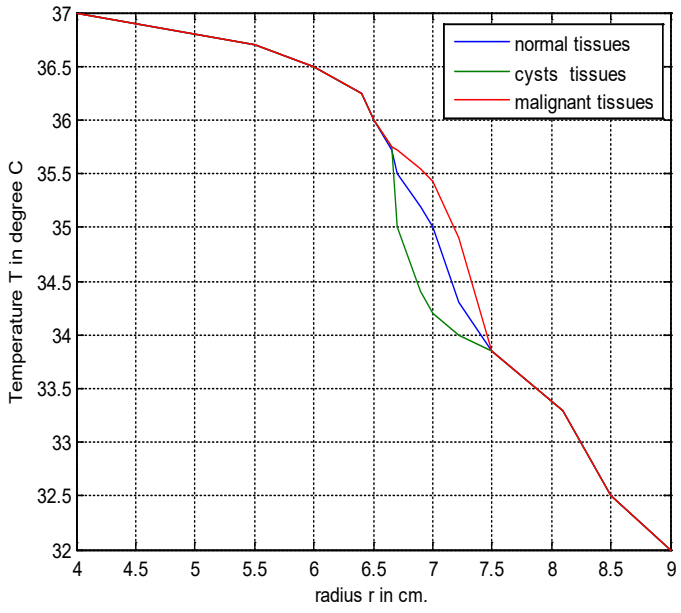

Fig.4. *Comparison of Temperature distribution in Cysts and malignant tumor with η=3.0 with normal tissues of Women's breast for Ta=230C, $E = 0.24 \times 10^{-3}$ gm/cm2min, Type-I boundary condition and case – 1 at θ= π/2*

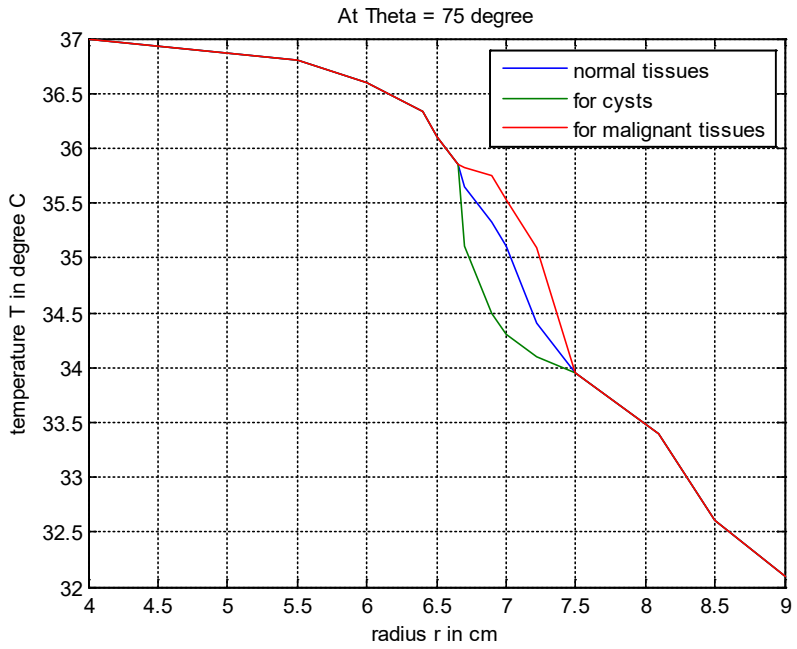

Fig.5. *Comparison of Temperature distribution in Cysts and malignant tumor with η=3.0 with normal tissues of Women's breast for* T_a*=23*^{0}*C,* $E = 0.24 \times 10^{-3}$ *gm/cm*^{2}*min, Type-I boundary condition and case – 1 at θ= 75*^{0}*C*

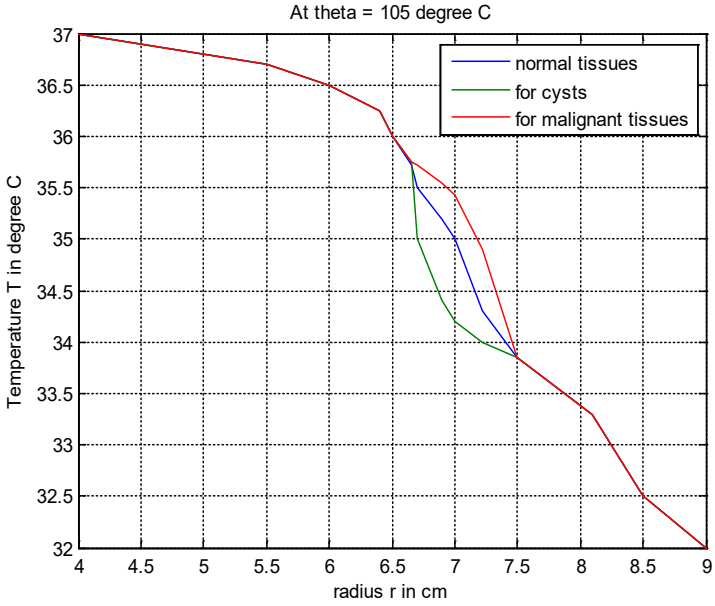

Fig.6. *Comparison of Temperature distribution in Cysts and malignant tumor with η=3.0 with normal tissues of Women's breast for* T_a*=23*^{0}*C,* $E = 0.24 \times 10^{-3}$ *gm/cm*^{2}*min, Type-I boundary condition and case – 1 at θ= 105*^{0}*C*

The temperature profiles coincide at *r=7.5* cm. and common temperature profile is observed from *r=7.5 to r=9.0 cm*. The figures 7 and 8 show the temperature profile for tumor and normal tissues and cysts at θ= 75ºC and θ= 105ºC respectively representing the cysts/ tumor at the angular position. The behavior of temperature profiles observed here is the same as that in figure 6. The fall in temperature in cysts is due to no metabolic activity in cysts whereas the elevation in temperature profiles in the malignant tumor is due to higher rate of metabolic activity in tumor [23,26].

The difference in temperature at various nodes in woman's breast due to presence and absence of lumps (cyst or tumor) for different atmospheric temperatures, different rates of evaporation, different sizes of cysts and different boundary conditions is shown in Tables 2, 3 and 4. In Table 2 we observe that difference is maximum at the central node of lumps (cyst or tumor) i.e. node no. 308 and these differences decrease with increase in distances from central node of the lumps (cyst or tumor) . The difference in temperature due to presence and absence of lumps at 306 and 310 is same due to symmetrical position of nodes in the lumps from central node of the lumps. Further we observe that maximum differences increase in Table -2 with increase in size of lumps. The similar observation can be made in Table 3 and 4. The maximum difference in temperature is observed due to presence and absence of cysts for Ta=15^0C and E=0 in comparison to that Table 2 and 3. This implies that the thermal disturbances in lumps (cyst or tumor) in woman's breast are more visible at lower atmospheric temperature as compared to that in Table-2 and 3 for higher atmospheric temperatures.

In Table 2,3 and 4 we observed that the temperature differences are slightly higher when lump is tumor as compare to the case when the lump is cyst. For tumor the max and min temperature differences found to be 0.765^0C and 0.245^0C. For cyst the max and min temperature differences found to be 0.735^0C and 0.225^0C respectively. the existing thermographic equipment is capable of measuring these temperature differences due to tumor and cyst with the normal tissues. The existing thermographic equipment is sensitive to temperature differences about 0.05^0C. Thus from the Table 2,3and 4 we can see that the smallest lump of 2mm diameter (1mm radius) can be detected in the both cases of being a cyst or a tumor by the existing thermographic equipment. Thus, there is significant difference in the behavior of temperature profiles of cysts and tumor regions. The slopes of the curve at the interfaces of normal tissues and cysts and normal tissues and tumor are significantly different. This information of behavior of temperature profiles in tumor and cyst region can be useful in distinguishing the tumor and cyst and preventing to false prediction rate of malignant tumors. The results obtained here have been compared with those obtained by Sudarshan et.al. and Osman et.al. and our results are very close of their results. The differences is in the results are due to difference in size and location of tumor in woman's breast. However, the results are also in agreement with biological facts. The information generated from such models can give us better insights for developing and standard for distinguishing tumor and cyst by thermography.

5. Machine Learning Validation of Computational Analysis of Malignant Tumors for Breast cancer

The aim of this study is to validate the obtained result by using thermal imaging as a potential tool for detecting breast cancer with machine learning approach. From the obtained result of this research we can say thermal information can be effectively used to distinguish between cysts and malignant tumor to prevent the false positive test of malignant tumor with the existing thermographic equipment the smallest lump of 2mm diameter (1mm radius) which may be a tumor or a cyst being present at a depth of 2.5 cm can be detect clearly. In this study, Mammographic Image Analysis Society (MIAS) database a benchmark dataset is considered for validation purpose, that already used by most of the researchers for validation of different developed algorithm [35]. The properties of dataset are shown in table one.

Table.2. Properties of dataset used.

Data sets	Number of extracted features	Cyst cases	Malignant cases
MIAS Dataset	**16**	**64**	**51**

After preprocessing and feature analysis classified the data with most popular classifier in this study for classification purpose, we considered ANN, SVM and Random forest classifiers [36-39]. After prepressing the dataset, we extracted the important features from the data set based on our research that are important for classification of cyst and malignant tumor. For training, the classifier considered 08 important features that are radius, perimeter, area, symmetry, texture, smoothness, compactness and concavity. The models trained with the best features were used for increasing testing accuracy of different classifiers. Table 1 depicted the best mean and worst classification accuracy of SVM, ANN and Random Forest classifiers.

Table.3. Depicted the classification accuracy of SVM, ANN and Random Forest classifiers used in cysts/malignant cases respectively.

	SVM	RF	ANN
Best Classification Accuracy (%)	**97.99**	**93.34**	**91.22**
Worst Classification Accuracy (%)	**95.33**	**87.77**	**96.55**
Mean Classification Accuracy (%)	**96.66**	**90.55**	**93.88**

Figure 7, 8 and 11of test data shows that SVM with linear kernel function is the most powerful, efficient, and accurate machine learning techniques compare to ANN and RF classifiers. Although other techniques performed very well in addition, they were able to accurately predict using selected feature by our analysis.. This indicate the ability to deal with few feature that selected on the basis of this computational research proposed in this paper..

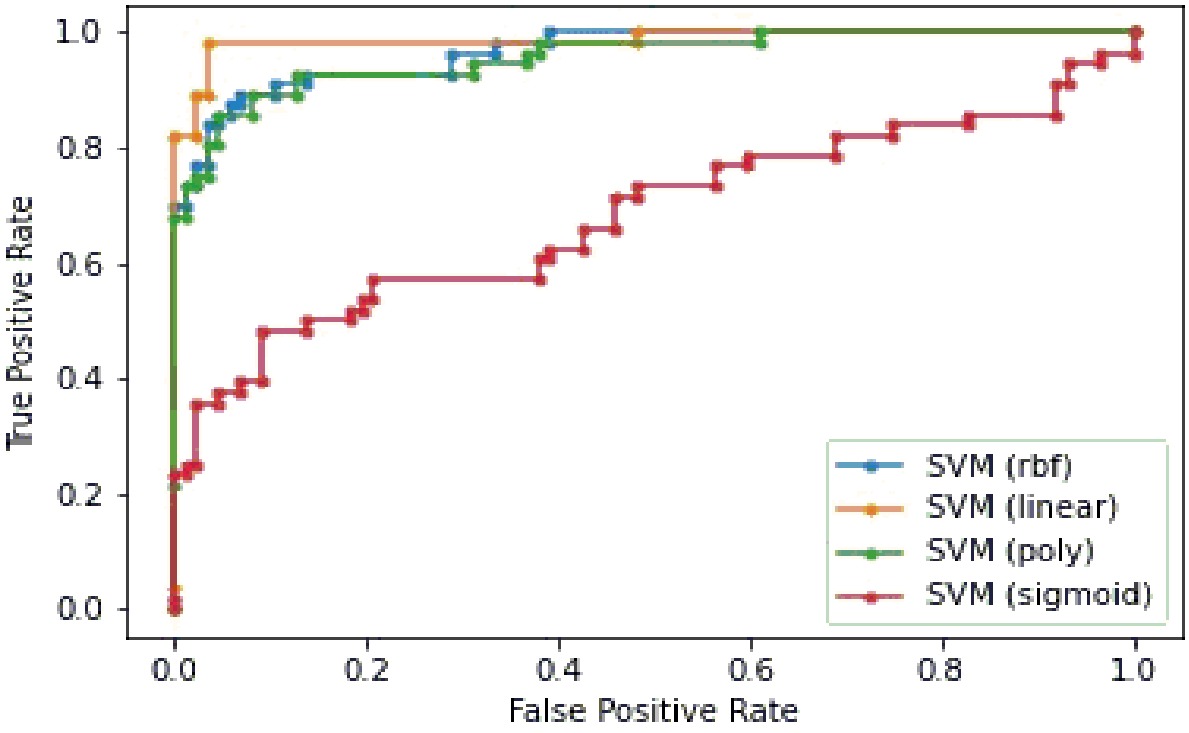

Fig.7. *The AUC curve for classification accuracy of SVM classifier with four-kernel function.*

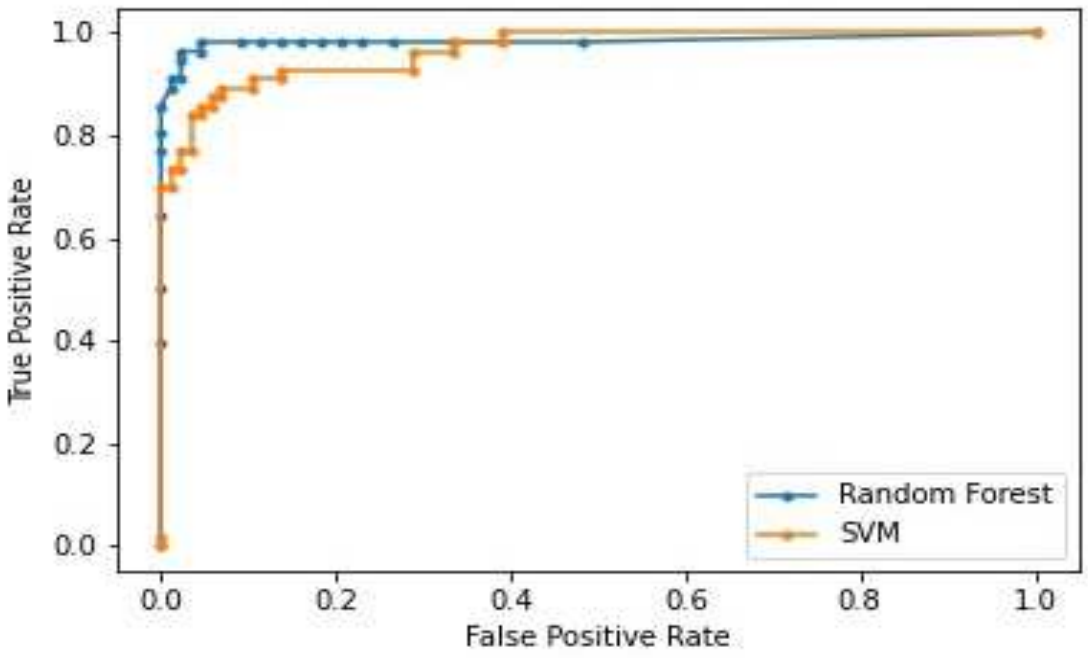

Fig.8. *The AUC curve for classification accuracy of Random Forest classifier and SVM classifier with Linear kernel function*

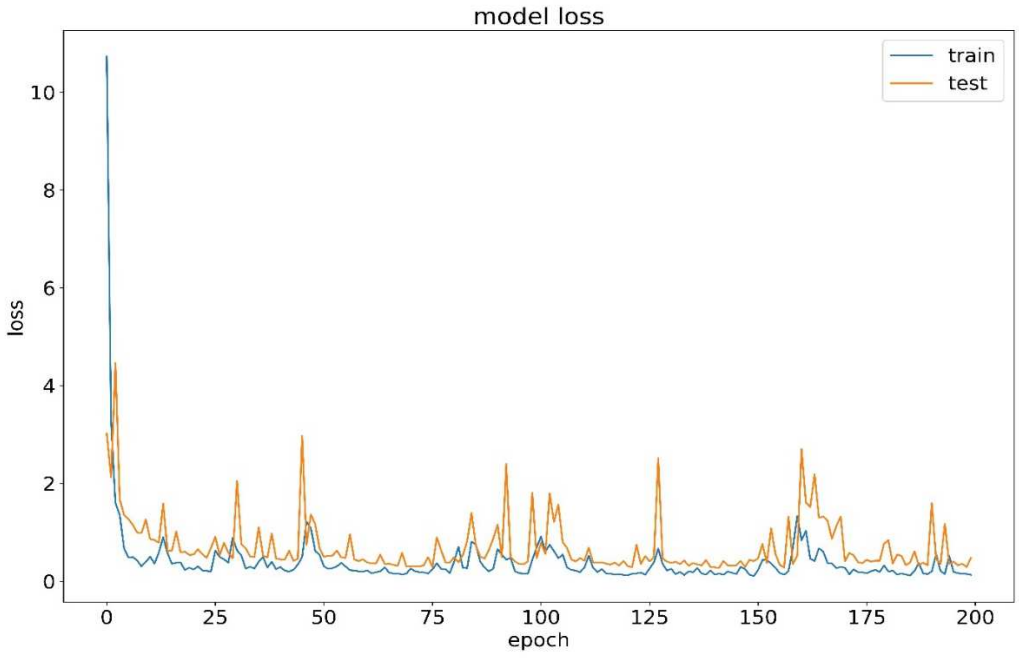

Fig.9. *For ANN classifier figure shown Model loss with different number of epoch.*

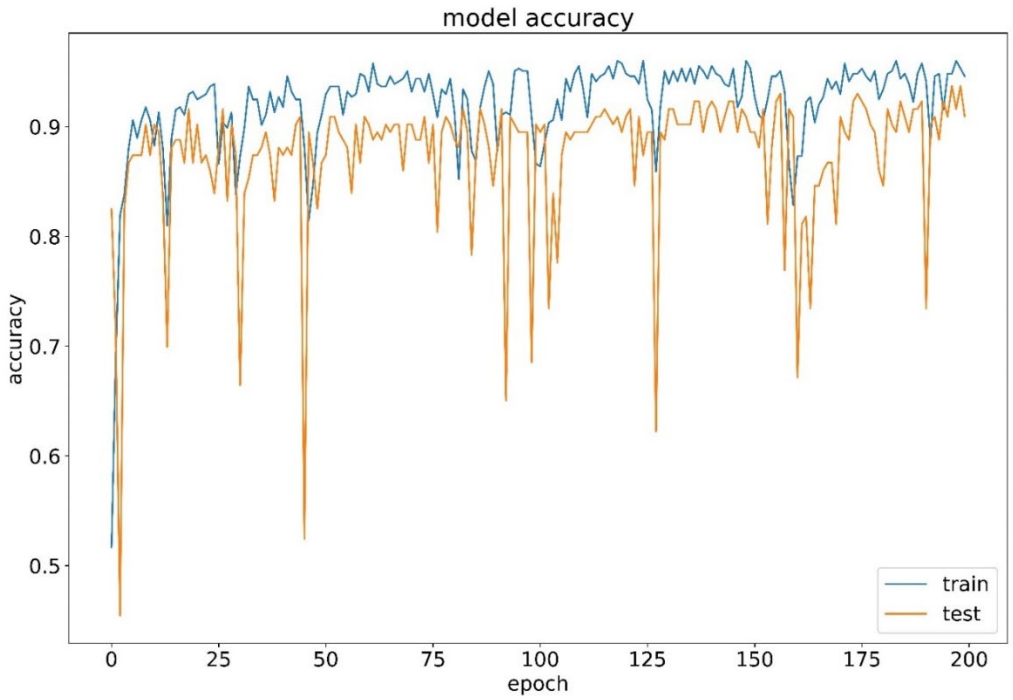

Fig.10. *For ANN classifier variation in classification accuracy with training and testing sets for different number of epoch.*

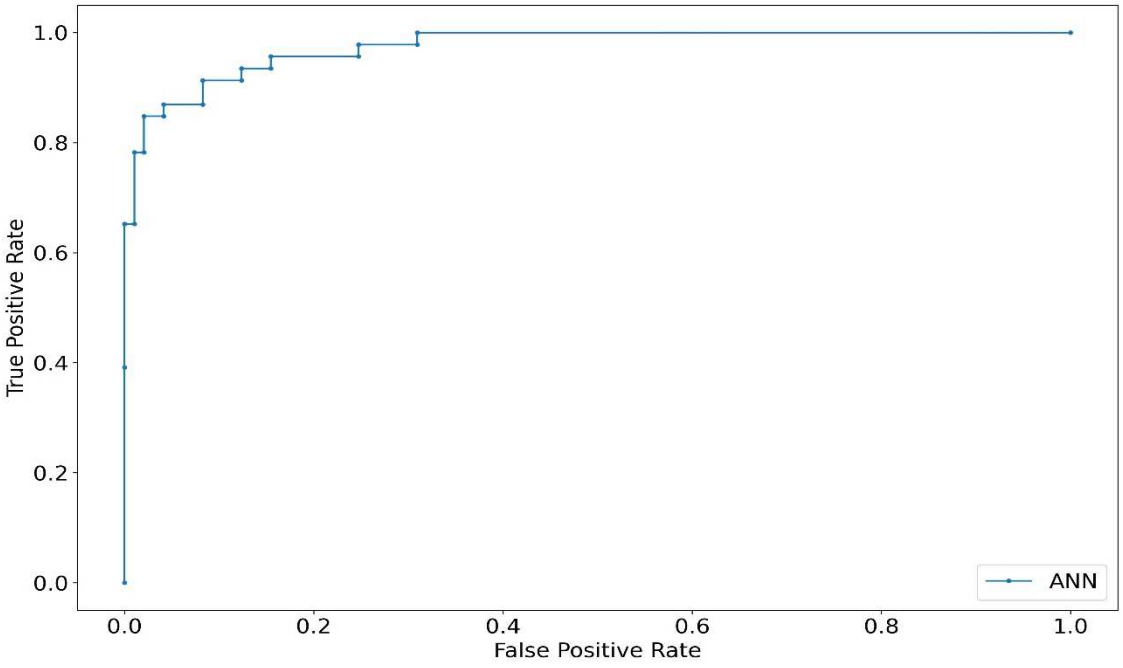

Fig.11. *The AUC curve for classification accuracy of ANN classifier*

Based on all experiments findings, figure 9 shows variation in classification accuracy with training and testing sets for different number of epoch for ANN classifier and figure 10 shows model loss with different number of epoch for ANN classifier.

6. Conclusion and Futuer Work

A two-dimensional finite element model is proposed and successfully employed to study the effect of cysts in comparison to malignant tissues in fat layers of women's breast. From the results it is concluded that the presence of cyst leads to fall in temperature in cyst region and surrounding tissues and presence of malignant tumor leads to elevation in temperature profiles in malignant tissues and surrounding region. The thermal effect of cyst and malignant tumor is just opposite in behavior in the women's breast. The slope of the curve at the junction of cysts and normal tissues is just opposite to the slope of the curve at the junction of malignant tissues and normal tissues. It is also concluded that the contrast in thermal behavior of cyst and tumor can be exploited in thermography for detection of cyst and tumors, their shape, size and location in woman's breast. Further this thermal information can be effectively used to distinguish between cysts and malignant tumor to prevent the false positive test of malignant tumor with the existing thermographic equipment the smallest lump of 2mm diameter (1mm radius) which may be a tumor or a cyst being present at a depth of 2.5 cm can be detect clearly. This study also concludes that compare to RF and ANN classifiers SVM is most powerful and efficient classification techniques for breast cancer classification, with selected features, which extracted by using done computational analysis.

These models can be developed further and simulated under various conditions to generate information, which can be useful for developing for standards for thermographic detection of lumps, which may be benign and malignant. The authors intend to carry out more research on thermal effect of benign disorder in comparison to malignant tumors in woman's breast to generate information for developing standards and protocols for the thermography. In all the research in this direction will be useful for biomedical scientist for effective thermal diagnosis of malignant and benign disorders in various human organs.

Declaration of interests (Conflict of Interest)

- The authors declare that they have no known competing financial interests or personal relationships that could have appeared to influence the work reported in this paper.
- The authors declare no Conflict of Interest.

Acknowledgement

Creators are appreciative to Science and Engineering Research Board, Department of Science and Technology, New Delhi, India for giving help to this work under NPDF-Scheme. Additionally, creators are grateful to Department of Biotechnology, New Delhi, India and M.P. board of Science and Technology, Bhopal, INDIA for giving Bioinformatics Infrastructure office at MANIT, Bhopal, INDIA to do this work.

Table.4. Difference in nodal temperatures due to presence and absence of cysts of different sizes at location -1, Type I Boundary Condition, $T_a=23^0C$ and different rates of evaporation

Rate of evaporation	Node Number	Temperature Differences							
		Case- For Small Lump with diameter 2 mm		Case -1 Lump with diameter 8.4 mm		Case -2 Lump with diameter 12 mm		Case -3 Lump with diameter 15 mm	
		Tumor	Cyst	Tumor	Cyst	Tumor	Cyst	Tumor	Cyst
$E=0.24X10^{-3}$	306	0.355	0.345	0.465	0.455	0.497	0.488	0.51	0.497
	307	0.415	0.408	0.52	0.512	0.537	0.529	0.552	0.537
	308	0.465	0.455	0.575	0.568	0.612	0.607	0.651	0.612
	309	0.415	0.408	0.52	0.512	0.557	0.552	0.552	0.557
	310	0.355	0.345	0.465	0.458	0.497	0.492	0.51	0.497
$E=0.48X10^{-3}$	306	0.375	0.365	0.485	0.478	0.517	0.5125	0.532	0.517
	307	0.435	0.428	0.545	0.541	0.5757	0.572	0.572	0.5757
	308	0.487	0.481	0.597	0.592	0.6452	0.615	0.671	0.6452
	309	0.435	0.428	0.545	0.541	0.5757	0.572	0.572	0.5757
	310	0.375	0.365	0.485	0.479	0.517	0.5125	0.532	0.517

Table.5. Difference in nodal temperatures due to presence and absence of cysts of different sizes at location -1, Type I Boundary Condition, $T_a=33^0C$ and different rates of evaporation

Rate of evaporation	Node Number	Temperature Differences							
		Case- For Lump with diameter 2 mm		Case -1 Lump with diameter 8.4 mm		Case -2 Lump with diameter 12 mm		Case -3 Lump with diameter 15 mm	
		Tumor	Cyst	Tumor	Cyst	Tumor	Cyst	Tumor	Cyst
$E=0.24X10^{-3}$	306	0.245	0.225	0.345	0.325	0.375	0.3685	0.405	0.395
	307	0.328	0.315	0.428	0.408	0.455	0.445	0.485	0.465
	308	0.411	0.398	0.511	0.499	0.521	0.505	0.54	0.524
	309	0.328	0.308	0.428	0.408	0.455	0.445	0.485	0.465
	310	0.245	0.225	0.345	0.325	0.375	0.3685	0.405	0.395
$E=0.48X10^{-3}$	306	0.265	0.245	0.365	0.345	0.389	0.369	0.412	0.392
	307	0.348	0.328	0.448	0.428	0.47	0.467	0.498	0.475
	308	0.431	0.411	0.531	0.511	0.545	0.5255	0.571	0.551
	309	0.348	0.328	0.448	0.428	0.47	0.467	0.498	0.475
	310	0.265	0.245	0.365	0.345	0.389	0.369	0.412	0.392
$E=0.72X10^{-3}$	306	0.279	0.255	0.379	0.359	0.409	0.399	0.429	0.408
	307	0.365	0.345	0.465	0.445	0.486	0.466	0.518	0.499
	308	0.45	0.435	0.55	0.53	0.561	0.541	0.589	0.565
	309	0.365	0.345	0.465	0.445	0.486	0.466	0.518	0.501
	310	0.279	0.255	0.379	0.359	0.409	0.399	0.429	0.402

Table.6. Difference in nodal temperatures due to presence and absence of cysts of different sizes at location -1 , Type II Boundary Condition, $T_a=15^0C$ and E=0

Rate of evaporation	Node Number	Temperature Differences							
		Case- For Lump with diameter 2 mm		Case -1 Lump with diameter 8.4 mm		Case -2 Lump with diameter 12 mm		Case -3 Lump with diameter 15 mm	
		Tumor	Cyst	Tumor	Cyst	Tumor	Cyst	Tumor	Cyst
E=0	306	0.385	0.379	0.495	0.489	0.55	0.525	0.63	0.613
	307	0.434	0.4285	0.54	0.505	0.59	0.569	0.67	0.647
	308	0.509	0.498	0.619	0.617	0.675	0.645	0.765	0.735
	309	0.423	0.418	0.54	0.505	0.59	0.569	0.67	0.647
	310	0.385	0.379	0.495	0.489	0.554	0.525	0.63	0.613

Table.7. Comparison of results with previous research workers

Location	Sudarshan's Result (^0C)	Osman Results (^0C)	Present Model Results(0C)
Surface temperature far away the tumor area	33.59	34.15	34.2

Surface temperature at focal point of tumor	34.8793	35.5	35.58
Temperature at limit point of tumor	33.9636	34.867	34.95

References

1. Onishi, N., et al., Ultrafast dynamic contrast-enhanced mri of the breast using compressed sensing: breast cancer diagnosis based on separate visualization of breast arteries and veins. 2018. 47(1): p. 97-104.
2. Chao, K. and W.J.B.-M.s. Yang, ASME, Response of skin and tissue temperature in sauna and steam baths. 1975: p. 69-71.
3. Aziz, R.M. Application of nature inspired soft computing techniques for gene selection: a novel frame work for classification of cancer. *Soft. Comput.* (2022). https://doi.org/10.1007/s00500-022-07032-9.
4. Chowdhary, C.L., et al., Decreasing false assumption for improved breast cancer detection. 2016. 35(2): p. 157-176.
5. Aziz RM. Nature-inspired metaheuristics model for gene selection and classification of biomedical microarray data. Medical & Biological Engineering & Computing. 2022 Apr 11:1-20.
6. Dobrolecki, L.E., et al., Patient-derived xenograft (PDX) models in basic and translational breast cancer research. 2016. 35(4): p. 547-573.
7. Makrariya, A. and N. Adlakha, Quantitative study of thermal disturbances due to nonuniformly perfused tumors in peripheral regions of women's breast. 2017. 16: p. 1176935117700894.

8. Makrariya, A., K.R.Pardasani, and Bioinformatics, Numerical study of the effect of non-uniformly perfused tumor on heat transfer in women's breast during menstrual cycle under cold environment. 2019. 8(1): p. 9.
9. Acharya, S., et al., Mathematical modeling of sex related differences in the sensitivity of the sweating heat responses to change in body temperature. 2016: p. 1-11.
10. Makrariya, A. and N.J.C.M.B.N. Adlakha, Thermographic pattern's in women's breast due to uniformly perfused tumors and menstrual cycle. 2019. 2019: p. Article ID 14.
11. Magalhaes, C., J. Mendes, and R.J.A.S. Vardasca, Meta-analysis and systematic review of the application of machine learning classifiers in biomedical applications of infrared thermography. 2021. 11(2): p. 842.
12. González, F.J.J.J.o.B.E., Thermal Simulations of Cancerous Breast Tumors and Cysts on a Realistic Female Torso. 2021. 143(6): p. 061001.
13. Makrariya, A., K.R.J.I.J.o.S. Pardasani, and P. Modelling, Numerical simulation of thermal changes in tissues of woman's breast during menstrual cycle in different stages of its development. 2019. 14(4): p. 348-359.
14. Soulami, K.B., et al., Detection of breast abnormalities in digital mammograms using the electromagnetism-like algorithm. 2019. 78(10): p. 12835-12863.
15. Makrariya, A., N. Adlakha, and S.K. Shandilya. 3D Spherical—Thermal Model of Female Breast in Stages of Its Development and Different Environmental Conditions. in Mathematical Modeling, Computational Intelligence Techniques and Renewable Energy: Proceedings of the First International Conference, MMCITRE 2020. 2021. Springer.
16. Hiley, C.T., et al., Challenges in molecular testing in non-small-cell lung cancer patients with advanced disease. 2016. 388(10048): p. 1002-1011.
17. Queiroz, K.F.F.d.C., et al., Developing and Using Computational Frameworks to Conduct Numerical Analysis and Calculate Temperature Profiles and to Classify Breast Abnormalities, in Biomedical Computing for Breast Cancer Detection and Diagnosis. 2021, IGI Global. p. 230-249.
18. dos Santos, W.P., W.W.A. da Silva, and M.A. de Santana, Biomedical Computing for Breast Cancer Detection and Diagnosis. 2020: Medical Information Science Reference.
19. Singh, S., R.J.E.b. Melnik, and medicine, Thermal ablation of biological tissues in disease treatment: A review of computational models and future directions. 2020. 39(2): p. 49-88.

20. Musheer, R.A., C. Verma, and N.J.S.C. Srivastava, Novel machine learning approach for classification of high-dimensional microarray data. 2019. 23(24): p. 13409-13421.
21. Aziz, R., C.K. Verma, and N. Srivastava, Artificial neural network classification of high dimensional data with novel optimization approach of dimension reduction. Annals of Data Science, 2018. 5(4): p. 615-635.
22. Hristov, J.J.F.i.P., Bio-heat models revisited: concepts, derivations, nondimensalization and fractionalization approaches. 2019. 7: p. 189.
23. Cooper, T.E. and G.J. Trezek, A probe technique for determining the thermal conductivity of tissue. 1972.
24. Michelotti, A., et al., Tackling the diversity of breast cancer related lymphedema: perspectives on diagnosis, risk assessment, and clinical management. 2019. 44: p. 15-23.
25. Kukuyan, A.-M., et al., Inactivation of Bap1 cooperates with losses of Nf2 and Cdkn2a to drive the development of pleural malignant mesothelioma in conditional mouse models. 2019. 79(16): p. 4113-4123.
26. Erzina, M., et al., Precise cancer detection via the combination of functionalized SERS surfaces and convolutional neural network with independent inputs. 2020. 308: p. 127660.
27. Taylor, N.A. and C.J.J.J.o.t.b. Gordon, The origin, significance and plasticity of the thermoeffector thresholds: Extrapolation between humans and laboratory rodents. 2019. 85: p. 102397.
28. Abaci, H., et al., Next generation human skin constructs as advanced tools for drug development. 2017. 242(17): p. 1657-1668.
29. Kandlikar, S.G., et al., Infrared imaging technology for breast cancer detection–Current status, protocols and new directions. 2017. 108: p. 2303-2320.
30. Ekici, S. and H.J.M.h. Jawzal, Breast cancer diagnosis using thermography and convolutional neural networks. 2020. 137: p. 109542.
31. Taktak, A., et al., Clinical engineering: a handbook for clinical and biomedical engineers. 2019: Academic Press.
32. Huang, Y., et al., Psychological resilience of women after breast cancer surgery: a cross-sectional study of associated influencing factors. 2019. 24(7): p. 866-878.
33. Naik, P.A.J.I.J.o.B., Modeling the mechanics of calcium regulation in T lymphocyte: a finite element method approach. 2020. 13(05): p. 2050038.

34. Ahmad, H., et al., Approximate Numerical solutions for the nonlinear dispersive shallow water waves as the Fornberg–Whitham model equations. 2021. 22: p. 103907.
35. Aziz R, Verma CK, Srivastava N. Dimension reduction methods for microarray data: a review. AIMS Bioengineering. 2017;4(2):179-97.
36. Aziz R, Verma CK, Srivastava N. A novel approach for dimension reduction of microarray. Computational biology and chemistry. 2017 Dec 1;71:161-9.
37. Aziz, R., N. Srivastava, and C.K. Verma, ISSN, T-independent component analysis for svm classification of dna-microarray data. 2015: p. 0975-3087.
38. Aziz, R., C. Verma, and N. Srivastava, A fuzzy based feature selection from independent component subspace for machine learning classification of microarray data. Genomics data, 2016. 8: p. 4-15.
39. Aziz, R., C. Verma, and N. Srivastava, A weighted-SNR feature selection from independent component subspace for nb classification of microarray data. 2015. 6: p. 245-255.
40 Aziz R, Verma CK, Jha M, Srivastava N. Artificial neural network classification of microarray data using new hybrid gene selection method. International Journal of Data Mining and Bioinformatics. 2017;17(1):42-65.
41 Musheer RA, Verma CK, Srivastava N. Novel machine learning approach for classification of high-dimensional microarray data. Soft Computing. 2019 Dec;23(24):13409-21.
42 Aziz RM, Baluch MF, Patel S, Ganie AH. LGBM: a machine learning approach for Ethereum fraud detection. International Journal of Information Technology. 2022 Jan 29:1-1.
43 Aziz RM, Hussain A, Sharma P, Kumar P. Machine learning-based soft computing regression analysis approach for crime data prediction. Karb Int J Mod Sci. 2022;8(1):1-9.
44 Desai NP, Baluch MF, Makrariya A, MusheerAziz R. Image processing Model with Deep Learning Approach for Fish Species Classification. Turkish Journal of Computer and Mathematics Education (TURCOMAT). 2022 Jan 12;13(1):85-99.

45 Aziz RM, Baluch MF, Patel S, Kumar P. A Machine Learning based Approach to Detect the Ethereum Fraud Transactions with Limited Attributes. Karbala International Journal of Modern Science. 2022;8(2):139-51.